Published in final edited form as:

Cancer Res. 2018 August 15; 78(16): 4704–4715. doi:10.1158/0008-5472.CAN-18-0399.

Mcl-1 phosphorylation without degradation mediates sensitivity to HDAC inhibitors by liberating BH3-only proteins

Jingshan Tong[1,2], **Xingnan Zheng**[1,3], **Xiao Tan**[1,2,4], **Rochelle Fletcher**[1,2], **Zaneta Nikolovska-Coleska**[5], **Jian Yu**[1,3], and **Lin Zhang**[1,2,*]

[1]UPMC Hillman Cancer Center, Pittsburgh, PA, 15213, USA.

[2]Department of Pharmacology and Chemical Biology, University of Pittsburgh School of Medicine, Pittsburgh, PA 15213, USA.

[3]Department of Pathology, University of Pittsburgh School of Medicine, Pittsburgh, PA 15213, USA.

[4]Department of Oncology, Xiangya Hospital, Central South University, Changsha, 410008, China.

[5]Department of Pathology, University of Michigan School of Medicine, Ann Arbor, MI 48109, USA.

Abstract

Mcl-1, a pro-survival Bcl-2 family protein, is frequently overexpressed in cancer cells and plays a critical role in therapeutic resistance. It is well known that anti-cancer agents induce phosphorylation of Mcl-1, which promotes its binding to E3 ubiquitin ligases and subsequent proteasomal degradation and apoptosis. However, other functions of Mcl-1 phosphorylation in cancer cell death have not been well characterized. In this study, we show in colon cancer cells that histone deacetylase inhibitors (HDACi) induce GSK3β-dependent Mcl-1 phosphorylation, but not degradation or downregulation. The *in vitro* and *in vivo* anticancer effects of HDACi were dependent on Mcl-1 phosphorylation and were blocked by genetic knock-in (KI) of a Mcl-1 phosphorylation site mutant. Phosphorylation-dead Mcl-1 maintained cell survival by binding and sequestering BH3-only Bcl-2 family proteins PUMA, Bim, and Noxa, which were upregulated and necessary for apoptosis induction by HDACi. Resistance to HDACi mediated by phosphorylation-dead Mcl-1 was reversed by small-molecule Mcl-1 inhibitors that liberated BH3-only proteins. These results demonstrate a critical role of Mcl-1 phosphorylation in mediating HDACi sensitivity through a novel and degradation-independent mechanism. These results provide new mechanistic insights on how Mcl-1 maintains cancer cell survival and suggest that Mcl-1-targeting agents are broadly useful for overcoming therapeutic resistance in cancer cells.

Keywords

Mcl-1; HDAC inhibitors; BH3-only proteins; colorectal cancer; apoptosis

[*]**Corresponding Author:** Lin Zhang, the UPCI Research Pavilion, Room 2.42a, 5117 Centre Ave., Pittsburgh, PA 15213. Phone: (412) 623-1009. Fax: (412) 623-7778. zhanglx@upmc.edu.

Conflict of interest: The authors have no conflict of interest.

Introduction

Stress-induced apoptosis in mammalian cells is regulated by the Bcl-2 family proteins. Pro-apoptotic BH3-only members such as PUMA, Bim and Noxa sense and become activated by different stress signals (1,2). They indirectly or directly activate the multi-BH domain containing proapoptotic members Bax/Bak, which triggers downstream events including mitochondrial outer membrane permeabilization (MOMP), cytosolic release of cytochrome *c*, and activation of caspases (1,2). Myeloid cell leukemia 1 (Mcl-1) is a pro-survival Bcl-2 family member that is frequently overexpressed or amplified in various human tumors (3). Mcl-1 suppresses apoptosis by binding to the BH3 domains of pro-apoptotic proteins through a hydrophobic surface groove to inhibit MOMP and caspase activation (4,5). A number of recent studies indicate a critical role of Mcl-1 in tumor cell survival and therapeutic resistance (5).

Mcl-1 protein stability and activity are regulated by post-translational modifications including phosphorylation (6). Mcl-1 protein contains a proline/glutamic acid/serine/threonine (PEST) region subjected to phosphorylation (3). Phosphorylation of Mcl-1 by glycogen synthase kinase 3β (GSK3β) or other kinases promotes the binding of Mcl-1 to E3 ubiquitin ligases including F-box and WD repeat domain-containing 7 (FBW7), Mule, and β-TrCP, leading to Mcl-1 ubiquitination and subsequent proteasomal degradation (7–9). Several studies using overexpressed Mcl-1 mutants suggest that Mcl-1 phosphorylation also affects its antiapoptotic activity and interactions with other Bcl-2 proteins (7,10,11). However, it remains unclear if and how Mcl-1 phosphorylation affects its endogenous function and interactions with other Bcl-2 family members and apoptosis.

Histone deacetylases (HDACs) are epigenetic enzymes that regulate gene expression by removing the acetyl group from histones. They are well-established targets in anticancer therapy (12,13). Several HDAC inhibitors (HDACi), such as suberoylanilide hydroxamic acid (SAHA; Vorinostat), have been approved for treating hematopoietic malignancies (12,13). However, HDACi as single agents are generally ineffective for solid tumors, and resistance to HDACi represents a major obstacle in their clinical applications (12). Induction of apoptosis has been implicated as a key effect of HDACi (14). HADCi-induced apoptosis was shown to require the BH3-only proteins Bim and Noxa in leukemia cells (15,16). Recent studies suggest that Mcl-1 is a major determinant of HADCi sensitivity in some leukemia and solid tumor cells (17–19). Nonetheless, how Mcl-1 mediates sensitivity and resistance to HDACi has remained unclear. The functional relationship between Mcl-1 and other Bcl-2 family proteins in therapeutic response to HDACi is obscure.

In this study, we used a genetic knock-in (KI) approach to identify a critical role of GSK3β-mediated Mcl-1 phosphorylation in apoptosis induced by HDACi in colon cancer cells. Our results demonstrate that Mcl-1 phosphorylation determines HDACi sensitivity by suppressing its bindings to PUMA, Bim, and Noxa, independent of ubiquitination and proteasomal degradation. They provide novel mechanistic insight on how Mcl-1 maintains cancer cell survival, and new clues for targeting Mcl-1 to overcome therapeutic resistance.

Materials and methods

Cell culture

Colon cancer cell lines, including HCT116, DLD1 and RKO, were obtained from the American Type Culture Collection (Manassas, VA). HCT116 cells with knock-in of the Mcl-1 phosphorylation site mutant S121A/E125A/S159A/T163A (*Mcl-1*-KI) were generated by homologous recombination as described (20). *PUMA*-knockout (KO) and *FBW7*-KO HCT116 and DLD1 cells were previously described (20,21). Cells were authenticated in 2017 by genotyping and analysis of protein expression by western blotting, and routinely checked for Mycoplasma contamination by PCR. All cell lines were maintained at 37°C in 5% CO_2 and cultured in McCoy's 5A modified media (Invitrogen) supplemented with 10% defined FBS (HyClone), 100 units/ml penicillin, and 100 μg/ml streptomycin (Invitrogen). For drug treatment, cells were plated in 12-well plates at 20–30% density 24 hr before treatment. DMSO (Sigma) stocks of SAHA, MS-275, SB216763, ABT-737, ABT-263, sunitinib, sorafenib, regorafenib, TW-37 (Selleck Chemicals), and Mcl-1 inhibitors including UMI-77 (22), UMI-212 (compound **21**), and UMI-36 (compound **36**) (23), were diluted to appropriate concentrations with cell culture medium.

Targeting *Bim* and *Noxa* in HCT116 cells

Gene targeting vectors were constructed by using the recombinant adeno-associated virus (rAAV) system (24). Briefly, two homologous arms flanking exon 2 of *Bim* or Noxa, along with a neomycin-resistant gene cassette (*Neo*), were inserted between two Not I sites in the AAV shuttle vector pAAV-MCS (Agilent Technologies). Packaging of rAAV was performed by using the AAV Helper-Free System (Agilent) according to the manufacturer's instructions. HCT116 cells containing two copies of *Bim* and *Noxa* were infected with the rAAV and selected by G418 (0.5 mg/ml, Mediatech) for 3 weeks. Drug-resistant clones were pooled and screened by PCR for targeting events with the following primers for *Bim*: P1, 5'-TGATTGGATGTATTCAGAGG/P2, 5'-CATTACTACAGCACTCTCCTC, or for *Noxa*: P1, 5'-GCGAAGGAAGTGGTGCATTG/P2, 5'-CTGAAGAAAACAGATGTGAGG, in combination with a primer for *Neo* 5'-TCTTGACGAGTTCTTCTGAG/5'-TTGTGCCCAGTCATAGCCG. Prior to targeting the second allele, the *Neo* cassette, which is flanked by Lox P sites, was excised from a heterozygous clone by infection with an adenovirus expressing Cre recombinase (Ad-Cre). Single clones were screened by PCR for *Neo* excision using P1/P2, and two independent positive clones were infected again with the *Bim*- or *Noxa*-targeting construct. After the second round, *Neo* was excised by Ad-Cre infection, and gene targeting was verified by PCR and western blotting.

MTS assay

Cells seeded in 96-well plates at a density of 1×10^4 cells/well were treated with SAHA or MS-275 for 72 hr. 3-(4,5-dimethylthiazol-2-yl)-5-(3-carboxymethoxyphenyl)-2-(4-sulfophenyl)-2H-tetrazolium (MTS) assay was performed using the MTS assay kit (Promega) according to the manufacturer's instructions. Chemiluminescence was measured by using a Wallac Victor 1420 Multilabel Counter (Perkin Elmer). Each assay was conducted in triplicate and repeated three times.

Western blotting

Western blotting was performed as previously described (25). Antibodies include those for PUMA, phospho-Mcl-1 (S159/T163), cleaved caspases 3, 8, and 9, ERK, phospho-ERK (T202/Y204), AKT, phospho-AKT (S473), GSK3β, phospho-GSK3β (S9), Bim, Noxa, Bad (Cell Signaling), V5, cytochrome oxidase subunit IV (Invitrogen), Bax, HA (Santa Cruz), Bcl-X_L, Mcl-1 (BD Biosciences), Bid (EMD Biosciences), cytochrome *c*, β-actin (Sigma), Bak (Millipore), and Bcl-2 (Dako), and FBW7 (Bethyl).

Transfection and siRNA knockdown

Transfection was performed using Lipofectamine 2000 (Invitrogen) according to the manufacturer's instructions. Expression constructs of HA-tagged PUMA, Bim and Noxa were previously described (25). *Mcl-1* expression construct was generated by cloning a PCR-amplified full-length human *Mcl-1* cDNA fragment into pcDNA3.1/V5-His vector (Invitrogen) (20). Mutations were introduced into *Mcl-1* using QuickChange XL site-directed mutagenesis kit (Agilent Technologies). siRNA transfection was done 24 hr before drug treatment using 200 pmol of control scrambled siRNA or human *Mcl-1* siRNA (CGCCGAATTCATTAATTTATT-dTdT) (Dharmacon).

Immunoprecipitation

After treatment, cells were harvested and re-suspended in 1 ml of EBC buffer (50 mM Tris-HCl, pH 7.5, 100 mM NaCl, 0.5% Nonidet P-40) supplemented with a protease inhibitor cocktail (Roche). Cell suspensions were sonicated and spun at 10,000×g for 10 min to prepare cell lysates. For immunoprecipitation (IP), 1–2 μg of IP antibodies were mixed with protein G/A-agarose beads (Invitrogen) for 20 min at room temperature. The beads were washed twice with PBS containing 0.02% Tween 20 (pH 7.4), incubated with cell lysates on a rocker for 6 hr at room temperature, and then washed three times with PBS (pH 7.4). Beads were then boiled in 2× Laemmli sample buffer and subjected to SDS-PAGE and western blot analysis.

Reverse transcription (RT) PCR

Total RNA was isolated using the Mini RNA Isolation II kit (ZYMO Research) according to the manufacturer's protocol. One-μg of total RNA was used to generate cDNA by the SuperScript II reverse transcriptase (Invitrogen). PCR was performed using previously described conditions (26). PCR primers include those for *PUMA*: 5'-CGACCTCAACGCACAGTACGA-3'/5'-AGGCACCTAATTGGGCTCCAT-3'; *Bim*: 5'-GGAGACGAGTTTAACGCTTAC-3'/5'-AAGCAAAATGTCTGCATGG-3'; *Noxa*: 5'-TTCAGCTCGCGTCCTGCAG-3'/5'-GTTCCTGAGCAGAAGAGTTTGG-3'; *Mcl-1*: 5'-ATGCTTCGGAAACTGGACAT-3'/5'-TGGAAGAACTCCACAAACCCA-3'; *FBW7*: 5'-GTGATAGAACCCCAGTTTCA-3'/5'-CCTCAGCCAAAATTCTCCAG-3'; *Mule*: 5'-CAGTTCCATAGAGCATTTGA-3'/5'-GCCATTCTCCTTTCCACCCC-3'; and *β-actin*: 5'-GACCTGACAGACTACCTCAT-3'/5'-AGACAGCACTGTGTTGGCTA-3'.

Analysis of apoptosis

Apoptosis was measured by counting condensed and fragmented nuclei after nuclear staining with Hoechst 33258 (Invitrogen) as previously described (25). At least 300 cells were analyzed for each sample. Colony formation assays were performed by plating treated cells in 12-well plates at appropriate dilutions, followed by crystal violet staining 14 days after plating as described (27). Each experiment was performed in triplicate and repeated at least twice. Annexin V/propidium iodide (PI) staining was performed using Annexin-Alexa Fluor 488 (Invitrogen) and PI as described (27). For analysis of cytochrome *c* release, cytoplasmic and mitochondrial fractions were separated by Mitochondrial Fractionation Kit (Active Motif) according to the manufacturer's instructions, followed by western blotting of cytochrome *c* in the cytoplasmic and mitochondrial fractions.

Xenograft tumor experiments

All animal experiments were approved by the University of Pittsburgh Institutional Animal Care and Use Committee. Female 5- to 6-week-old Nu/Nu mice (Charles River) were housed in micro isolator cages in a sterile environment, and allowed access to water and chow *ad libitum*. Xenograft tumors were established by subcutaneously injecting mice with 4×10^6 of WT or *Mcl-1*-KI HCT116 cells. After tumor growth for 7 days, mice were treated daily for 10 consecutive days with SAHA (50 mg/kg/d) or the control vehicle. Tumor volumes were measured by calipers and calculated according to the formula 1/2 × length × width^2. After tumors reached 1.0 cm^3 in size, mice were euthanized and tumors were dissected and fixed in 10% formalin and embedded in paraffin. Terminal deoxynucleotidyl transferase mediated dUTP Nick End Labeling (TUNEL; Millipore) and active caspase 3 (Cell Signaling) immunostaining was performed on 5-mm paraffin-embedded tumor sections. Signals were detected by Alexa Fluor 488- (for TUNEL) or Alexa Fluor 594-conjugated (for active caspase 3) secondary antibodies (Invitrogen) with nuclear counter staining by 4' 6-Diamidino-2-phenylindole (DAPI).

Interactions of PUMA and Mcl-1 were detected by *in situ* proximity ligation assay (PLA) in paraffin-embedded sections of WT or *Mcl-1*-KI HCT116 tumor tissues from nude mice treated with SAHA for 1 day. PLA was performed using the Duolink *In Situ* Red Starter Kit (Sigma) according to the manufacturers' instructions. The sections were incubated with PUMA (rabbit, 1:50; Abcam) and Mcl-1 (mouse, 1:100; BD Biosciences) antibodies for at 4°C overnight, and then mounted with Vectashield Mounting Medium (Vector Laboratories) with DAPI (Sigma) for nuclear counter staining. PLA signals were visualized by fluorescence microscopy (Olympus) and quantified by counting.

Statistical analysis

Statistical analysis was carried out using GraphPad Prism VI software. *P* values were calculated by the student's t-test and were considered significant if $P < 0.05$. Means ± standard deviation (s.d.) were displayed in the figures.

Results

HDACi induce GSK3β-dependent Mcl-1 phosphorylation and apoptosis, but not Mcl-1 degradation or downregulation, in colon cancer cells

We recently showed that treating HCT116 colon cancer cells with a multi-kinase inhibitor, such as regorafenib, sorafenib, UCN-01, or sunitinib, induced S159/T163 phosphorylation of Mcl-1, which is essential for Mcl-1 ubiquitination, proteasomal degradation, and subsequent apoptosis induction (20). In addition to the kinase inhibitors, the HDACi SAHA and MS-275 were also found to induce Mcl-1 phosphorylation (Fig. 1A), which correlated with apoptosis induction (Fig. 1B, right panel). However, unlike the kinase inhibitors, HDACi treatment did not promote Mcl-1 degradation as shown by unchanged Mcl-1 protein expression (Fig. 1, A and C) and half-life (Fig. S1A). *Mcl-1* mRNA expression was slightly increased in response to SAHA, but unchanged after MS-275 treatment (Fig. S1B). HDACi treatment also induced Mcl-1 phosphorylation without degradation in DLD1 and RKO colon cancer cells, and even increased total Mcl-1 level in DLD1 cells after 16 hours (Fig. S1, C and D). These intriguing observations suggest that the level of total Mcl-1 may not be the key determinant of its activity, and prompted us to further investigate the mechanism and functional role of Mcl-1 phosphorylation in HDACi-induced apoptosis.

HDACi-induced Mcl-1 phosphorylation requires GSK3β, and could be blocked by the GSK3 inhibitor SB216763 or *GSK3β* knockdown by siRNA of (Fig. 1B, left panel and S1E, left panel). SAHA or MS-275 treatment reduced ERK phosphorylation (T202/Y204), and relived ERK-mediated inhibitory phosphorylation (S9) of GSK3β (Fig. 1A) (28). Mcl-1 phosphorylation by GSK3β or other kinases was shown to involve 3 sites including S121, S159, and T163 (8,9). Phosphorylation-mediated binding of Mcl-1 to FBW7 could be blocked by a quadruple mutant of these 3 sites and the phospho-mimic site E125 (4A mutant: S121A/E125A/S159A/T163A) (9). Transfection of the 4A mutant (20), not wild-type (WT) Mcl-1, completely blocked SAHA- and MS-275-induced Mcl-1 phosphorylation (Fig. 1D). Furthermore, GSK3β inhibition or knockdown suppressed apoptosis induced by SAHA or MS-275 (Fig. 1B, right panel and S1E, right panel). Compared to WT Mcl-1, the 4A mutant Mcl-1 expressed at a similar level had the stronger effect of suppressing HDACi-induced apoptosis in HCT116 cells (Fig. 1E), which was confirmed in DLD1 and RKO cells (Fig. S1, F and G). These results suggest a critical role GSK3β-mediated Mcl-1 phosphorylation in apoptotic response to HDACi.

Knock-in (KI) of Mcl-1 phosphorylation site mutant suppresses HDACi-induced apoptosis

We used a genetic knock-in (KI) approach to further delineate the functional role of Mcl-1 phosphorylation independent of degradation (Fig. S2A). HCT116 cells with KI of Mcl-1 phosphorylation site mutant (*Mcl-1*-KI) (20) were completely resistant to SAHA- and MS-275-induced phosphorylation (Fig. 1F), and had suppressed nuclear fragmentation (Fig. 2A), and increased viability (Fig. 2B) and clonogenic survival (Fig. 2C). Blocked apoptosis was further confirmed by reduced Annexin V staining (Fig. S2B), caspase 3, 8 and 9 activation (Fig. 2D) and cytochrome *c* release (Fig. 2E). Consistent with Mcl-1 dependency, knockdown of *Mcl-1* restored SAHA and MS-275 sensitivity in *Mcl-1*-KI cells (Fig. 2A, 2B and S2B). *Mcl-1*-KI cells were also resistant to the kinase inhibitors that induce Mcl-1

degradation, including regorafenib, sorafenib, UCN-01, and sunitinib (Fig. S2C) (20), but remained sensitive to other anticancer agents such as TRAIL, etoposide, and sulindac (20). These results demonstrate that Mcl-1 phosphorylation, but not its degradation, is critical for HDACi-induced apoptosis.

To better understand unaltered Mcl-1 stability in response to HDACi, we examined the E3 ubiquitin ligases of Mcl-1, including FBW7 and Mule. SAHA or MS-275 at the apoptosis-inducing concentration did not affect the expression of *FBW7* and *Mule*, in contrast to their marked induction by regorafenib and sorafenib (Fig. S3, A-C). SAHA- and MS-275-induced apoptosis was not suppressed, but slightly enhanced in isogenic *FBW7*-knockout (KO) HCT116 and DLD1 cells, which had reduced apoptotic response to regorafenib and other kinase inhibitors (Fig. S3, D and E) (20). Furthermore, transfection of WT *FBW7*, but not the tumor-derived inactivating mutants including R465C and R505C (29), was sufficient to promote Mcl-1 degradation in HDACi-treated HCT116 cells (Fig. S3F), indicating that insufficient expression of FBW7 or other Mcl-1 E3 ligases is responsible for the lack of Mcl-1 degradation in response to HDACi. These results suggest that depending on specific stimuli and whether an E3 ligase of Mcl-1 is induced, Mcl-1 phosphorylation can promote apoptosis through a degradation-dependent or -independent mechanism.

PUMA, Bim and Noxa are induced and required for HDACi-induced apoptosis

To determine how Mcl-1 phosphorylation mediates HDACi-induced apoptosis, we analyzed other Bcl-2 family members. Interestingly, we found that three BH3-only proteins, including PUMA, Bim and Noxa, were all induced in response to HDACi treatment (Fig. 3A and S1C). *PUMA*, *Bim* and *Noxa* mRNA expression was also markedly elevated following SAHA or MS-275 treatment (Fig. S4, A-C). In contrast, other proapoptotic and antiapoptotic members, including Bad, Bid, Bax, Bak, Bcl-2, and Bcl-X_L, were not substantially altered in response to SAHA and MS-275 treatment (Fig. 3A).

We then analyzed isogenic HCT116 cells with KO of *PUMA* (21), *Bim* (Fig. S4D), or *Noxa* (Fig. S4E) to determine whether the induced BH3-only proteins are necessary for HDACi-induced apoptosis. Indeed, deletion of *PUMA*, *Bim* or *Noxa* led to substantially increased cell viability (Fig. 3B), decreased nuclear fragmentation (Fig. 3C) and Annexin V staining (Fig. S5A), blocked activation of caspases 3 and 9 (Fig. 3D), and markedly improved clonogenic survival (Fig. 3E), in response to SAHA or MS-275. Decreased sensitivity to HDACi was also observed in *PUMA*-KO DLD1 cells (Fig. S5B). Consistent with the functions of BH3-only proteins in activating Bax and/or Bak, HDACi-induced apoptosis and caspase activation were suppressed in *BAX*-KO HCT116 cells (Fig. S5, C and D). Therefore, HDACi induces apoptosis in colon cancer cells by upregulating multiple BH3-only proteins, which cooperatively activate Bax to cause caspase activation.

Phosphorylation-dead Mcl-1 binds to PUMA, Bim, and Noxa to inhibit cell death, which is abrogated by small-molecule Mcl-1 inhibitors

We further investigated if Mcl-1 phosphorylation regulates the activity of BH3-only proteins in HDACi-induced apoptosis through protein-protein interactions. Following SAHA treatment, phosphorylation-dead Mcl-1 showed markedly enhanced binding to PUMA, Bim

and Noxa (Fig. 4A), which led to reduced interaction of Bcl-X_L with PUMA, Bim and Noxa, but increased interaction of Bcl-X_L with Bax (Fig. 4B). These differences in binding were confirmed by reciprocal IP using anti-Bim or anti-Noxa antibody (Fig. S6, A and B). Similar changes were observed in MS-275-treated cells (Fig. S6C). To further determine how Mcl-1 phosphorylation affects the binding to BH3-only proteins, WT or the 4A mutant Mcl-1, along with PUMA, Bim or Noxa, was transfected into HCT116 cells. IP analysis revealed that the mutant Mcl-1 bound to substantially more PUMA, Bim and Noxa compared to WT Mcl-1 (Fig. 4C), indicating an intrinsic difference in binding capacity to BH3-only proteins between WT and the mutant Mcl-1. Furthermore, inhibiting Mcl-1 phosphorylation by the GSK3 inhibitor SB216763 enhanced the binding of endogenous Mcl-1 to PUMA, Bim, and Noxa (Fig. 4D). Because E125 is a phospho-mimic but not a phosphorylation site, we also generated and analyzed the E125A mutant, and found this mutant did not affect the binding of Mcl-1 to PUMA and Bim (Fig. S6D). Together, our data suggest that Mcl-1 phosphorylation liberates PUMA, Bim and Noxa upon their induction, and allows them to bind to Bcl-X_L or other pro-survival factors to promote apoptosis.

Mcl-1 phosphorylation is likely compromised in drug-resistant cancer cells due to insufficient GSK3β activity caused by aberrant ERK activation. We therefore tested if HDACi resistance mediated by the lack of Mcl-1 phosphorylation could be overcome by direct inhibition of Mcl-1. Indeed, treating cells with an Mcl-1-selective small-molecule inhibitor, including UMI-77 (22), UMI-212, or UMI-36 (23), or the pan-Bcl-2 inhibitor TW-37 with a strong effect on Mcl-1 (30), restored SAHA- and MS-275-induced apoptosis and caspase activation in *Mcl-1*-KI cells (Fig. 5A, 5B, and S7). IP analysis showed TW-37 treatment restored the binding of endogenous PUMA, Bim and Noxa to Bcl-X_L (Fig. 5C). These results suggest that Mcl-1 inhibitors could be useful for enhancing the sensitivity to anticancer agents such as HDACi, which induce Mcl-1 phosphorylation but not degradation.

Mcl-1 phosphorylation without degradation mediates the anti-tumor effects of SAHA *in vivo*

We then used xenograft models to analyze the *in vivo* effects of Mcl-1 phosphorylation and HDACi sensitivity. Compared to WT HCT116 tumors, *Mcl-1*-KI tumors were significantly more resistant to SAHA treatment (Fig. 6, A and B). Apoptosis was markedly reduced in *Mcl-1*-KI tumors compared to WT tumors as indicated by TUNEL and active caspase 3 staining (Fig. 6, C and D). Consistent with the findings from cultured cells, SAHA treatment did not cause Mcl-1 degradation, but induced the expression of PUMA, Bim and Noxa in WT and *Mcl-1*-KI xenograft tumors (Fig. 6E). Probing *in situ* protein-protein interactions by proximity ligation assay (PLA) (31) revealed significantly enhanced interaction between the mutant Mcl-1 and PUMA in *Mcl-1*-KI tumors (Fig. 6F). These results confirmed the pivotal role of Mcl-1 phosphorylation in mediating the *in vivo* antitumor effects of HDACi by liberating PUMA and other BH3-only proteins, independent of Mcl-1 degradation.

Discussion

A hallmark of cancer is resistance to apoptosis, which maintains survival of cells *en route* to oncogenic transformation (32). Overexpression or amplification of *Mcl-1* is one of the most

frequent alterations in human cancers and underlies development of therapeutic resistance by evading cell death (33). Among the antiapoptotic Bcl-2 family proteins, Mcl-1 regulation is uniquely dynamic and complex. Mcl-1 harbors a long unstructured N-terminus containing the PEST region which includes many phosphorylation sites. Phosphorylation of Mcl-1 at these sites by GSK3β, p38, JNK, CDK1, casein kinase II, or other kinases may have a variety of functional roles in apoptosis induced by different stress conditions including therapeutic treatment (7–9).

Our study provides convincing evidence that drug-induced Mcl-1 phosphorylation directly affects the interactions of Mcl-1 with multiple BH3-only proteins to inhibit other antiapoptotic members and activate Bax/Bak. Our biochemical and genetic data demonstrate that HDACi require Mcl-1 phosphorylation by GSK3β on at least 3 sites, including S121, S159, and T163, to induce apoptosis in colon cancer cells. The E125 site analyzed in the 4A mutant and *Mcl-1*-KI cells had no effect on these interactions. Mcl-1 phosphorylation unleashes the full pro-apoptotic activity of PUMA, Bim and Noxa, and allows them to bind to and neutralize other pro-survival factors such as Bcl-X_L, which plays a key role in colon cancer cell survival (34). This is contrast to apoptosis induced by the kinase inhibitors, which largely relies on a single BH3-only protein PUMA (20), but is enhanced by *FBW7*-mediated Mcl-1 degradation to achieve a threshold level for cell death. Therefore, whether Mcl-1 degradation is necessary for apoptosis induction may be determined by the strength of BH3 signals and the induction of *FBW7* or other E3 ligases (Fig. 7). If the BH3 signal is strong enough, such as in cases where multiple BH3-only proteins are induced, Mcl-1 only needs to be phosphorylated to release sufficient BH3 signals to inactivate key pro-survival factors to induce cell death. If the BH3 signal is not very strong, such as when a single BH3-only protein is activated, an E3 ligase needs to be activated to promote Mcl-1 degradation for unleashing sufficient BH3 signal for cell killing (Fig. 7).

There are a number of published three-dimensional structures of the complexes formed between Mcl-1 and BH3 domains of BH3-only proteins, including PUMA, Bim and Noxa (35–37). All of these structures were obtained from recombinant Mcl-1 with deletions of N-terminal 153 residues including the PEST region, as well as the C-terminal 11 or 23 residues including the transmembrane anchor. The Mcl-1 protein used in these studies retains the BH3 binding groove and thus the binding affinity and selectivity for the BH3 peptides derived from BH3-only proteins (36,38). While these complex structures provided essential knowledge about the interactions in the BH3 domain, they are not informative for the interactions between the PEST region and BH3-only proteins, which can be used as a template to build a model to provide insights on the interactions between the mutant Mcl-1 and BH3-only proteins. However, it is well established that post-translational modifications such as phosphorylation are specifically recognized by interacting proteins, and can modulate the strength of the interactions, conformational changes, steric constraints, and thus potentially affecting the protein-protein interactions (39–41). Indeed, in *Mcl-1*-KI cells, phosphorylation-deficient Mcl-1 has increased binding to PUMA, Bim and Noxa, which frees Bcl-X_L and other antiapoptotic proteins to more efficiently inhibit Bax/Bak. In line with our findings, several previous studies using transfected mutant Mcl-1 suggest that Mcl-1 phosphorylation has other effects, in addition to promoting the binding to E3 ligases and degradation. For example, co-phosphorylation of S121 and T163 impaired its

antiapoptotic function in response to H_2O_2 treatment (11). GSK3-mediated phosphorylation at S159 inhibits the interaction of Mcl-1 with Bim (7). Co-phosphorylation of Mcl-1 at S159 and T163 was shown to reduce the antiapoptotic function of Mcl-1 (10). Our results reveal the relevant context for further investigating the degradation-independent function of Mcl-1 phosphorylation that might be amenable for drug development and optimization. However, it should be noted that the observed effects of HDACi on Mcl-1 may not be generalizable to all cell types, as the mechanisms of apoptosis are dependent on cell types and cellular contexts. For example, Mcl-1 accumulation caused by FBW7 deficiency had opposite effects on sorafenib-induced apoptosis in colon cancer cells and T-cell acute lymphoblastic leukemia cells (8,29).

SAHA and other HDACi are approved by the U.S. Food and Drug Administration for use in cutaneous T-cell leukemia (12,13). However, HDACi alone are not effective for treating solid tumors. Overexpression of Bcl-2 has previously been shown to cause HADCi resistance (12). The dependence on Mcl-1 phosphorylation suggests Mcl-1 as a critical mediator of HDACi sensitivity and resistance. Similar to our findings, previous studies showed that SAHA induces PUMA, Bim, and Noxa, and that Mcl-1 is a dominant pro-survival factor in head and neck squamous cell carcinoma (HNSCC) cells (19). In this case, *FBW7* mutations also did not protect, but sensitize HNSCC cells to SAHA, which may be due to the effects of FBW7 on other substrates such as Jun, Myc, cyclin E, and notch 1 (42). SAHA has synergy with BH3 mimetics in killing HNSCC cells (19), also suggesting a threshold level of BH3 signal as the key determinant of SAHA sensitivity. In leukemia cells, PUMA, Bim and Noxa could also be induced by SAHA (16). However, only Bim, but not PUMA and Noxa, was required for SAHA-induced apoptosis (16), reflecting the cell type specific function of these proteins. Furthermore, the E3 ubiquitin ligase Mule was shown to mediate HDACi sensitivity in MEF cells by promoting the ubiquitination and degradation of HDAC2 (43). These findings further support the critical role of Bcl-2 family in HDACi-induced therapeutic response and cancer type-specific resistance mechanisms.

Inhibiting pro-survival Bcl-2 family proteins in tumor cells has emerged as an attractive therapeutic strategy, leading to recent approval of the Bcl-2-selective inhibitor ABT-199 (Venetoclax) for the treatment of chronic lymphocytic leukemia (44). However, ABT-199 and related agents do not bind to Mcl-1, and resistance to these agents quickly emerges due to overexpression of Mcl-1 (45–47). There is an urgent need for developing small-molecule Mcl-1 inhibitors. Several different chemical classes of Mcl-1 inhibitors have been described (22,48,49). Our data suggest that Mcl-1-binding BH3 mimetics can be used to overcome therapeutic resistance caused by compromised Mcl-1 phosphorylation. Mcl-1 inhibitors may be broadly useful for potentiating many anticancer agents that promote Mcl-1 phosphorylation, even without a change in Mcl-1 stability or expression. The isogenic *Mcl-1*-KI cells lacking drug-induced phosphorylation can help identify new inhibitors or drug combinations with improved potency and on-target activity.

Supplementary Material

Refer to Web version on PubMed Central for supplementary material.

Acknowledgements

We thank our lab members for critical reading and discussion. This work is supported by U.S. National Institute of Health grants (R01CA172136 and R01CA203028 to L. Zhang; U19AI068021 R01CA215481 to J. Yu; R01CA149442 to Z. Nikolovska-Coleska; R01CA217141 to Z. Nikolovska-Coleska and L. Zhang). This project used the UPMC Hillman Cancer Center shared facilities that were supported in part by award P30CA047904.

References

1. Moldoveanu T, Follis AV, Kriwacki RW, Green DR. Many players in BCL-2 family affairs. Trends in biochemical sciences 2014;39(3):101–11. [PubMed: 24503222]
2. Bhola PD, Letai A. Mitochondria-Judges and Executioners of Cell Death Sentences. Mol Cell 2016;61(5):695–704. [PubMed: 26942674]
3. Thomas LW, Lam C, Edwards SW. Mcl-1; the molecular regulation of protein function. FEBS Lett 2010;584(14):2981–9. [PubMed: 20540941]
4. Youle RJ, Strasser A. The BCL-2 protein family: opposing activities that mediate cell death. Nat Rev Mol Cell Biol 2008;9(1):47–59. [PubMed: 18097445]
5. Perciavalle RM, Opferman JT. Delving deeper: MCL-1's contributions to normal and cancer biology. Trends in cell biology 2013;23(1):22–9. [PubMed: 23026029]
6. Mojsa B, Lassot I, Desagher S. Mcl-1 ubiquitination: unique regulation of an essential survival protein. Cells 2014;3(2):418–37. [PubMed: 24814761]
7. Maurer U, Charvet C, Wagman AS, Dejardin E, Green DR. Glycogen synthase kinase-3 regulates mitochondrial outer membrane permeabilization and apoptosis by destabilization of MCL-1. Mol Cell 2006;21(6):749–60. [PubMed: 16543145]
8. Inuzuka H, Shaik S, Onoyama I, Gao D, Tseng A, Maser RS, et al. SCF(FBW7) regulates cellular apoptosis by targeting MCL1 for ubiquitylation and destruction. Nature 2011;471(7336):104–9. [PubMed: 21368833]
9. Wertz IE, Kusam S, Lam C, Okamoto T, Sandoval W, Anderson DJ, et al. Sensitivity to antitubulin chemotherapeutics is regulated by MCL1 and FBW7. Nature 2011;471(7336):110–4. [PubMed: 21368834]
10. Ding Q, He X, Hsu JM, Xia W, Chen CT, Li LY, et al. Degradation of Mcl-1 by beta-TrCP mediates glycogen synthase kinase 3-induced tumor suppression and chemosensitization. Mol Cell Biol 2007;27(11):4006–17. [PubMed: 17387146]
11. Inoshita S, Takeda K, Hatai T, Terada Y, Sano M, Hata J, et al. Phosphorylation and inactivation of myeloid cell leukemia 1 by JNK in response to oxidative stress. J Biol Chem 2002;277(46):43730–4. [PubMed: 12223490]
12. Lee JH, Choy ML, Marks PA. Mechanisms of resistance to histone deacetylase inhibitors. Advances in cancer research 2012;116:39–86. [PubMed: 23088868]
13. West AC, Johnstone RW. New and emerging HDAC inhibitors for cancer treatment. J Clin Invest 2014;124(1):30–9. [PubMed: 24382387]
14. Zhang J, Zhong Q. Histone deacetylase inhibitors and cell death. Cell Mol Life Sci 2014;71(20): 3885–901. [PubMed: 24898083]
15. Inoue S, Riley J, Gant TW, Dyer MJ, Cohen GM. Apoptosis induced by histone deacetylase inhibitors in leukemic cells is mediated by Bim and Noxa. Leukemia 2007;21(8):1773–82. [PubMed: 17525724]
16. Chen S, Dai Y, Pei XY, Grant S. Bim upregulation by histone deacetylase inhibitors mediates interactions with the Bcl-2 antagonist ABT-737: evidence for distinct roles for Bcl-2, Bcl-xL, and Mcl-1. Mol Cell Biol 2009;29(23):6149–69. [PubMed: 19805519]
17. Pierceall WE, Lena RJ, Medeiros BC, Blake N, Doykan C, Elashoff M, et al. Mcl-1 dependence predicts response to vorinostat and gemtuzumab ozogamicin in acute myeloid leukemia. Leuk Res 2014;38(5):564–8. [PubMed: 24636337]
18. Inoue S, Walewska R, Dyer MJ, Cohen GM. Downregulation of Mcl-1 potentiates HDACi-mediated apoptosis in leukemic cells. Leukemia 2008;22(4):819–25. [PubMed: 18239621]

19. He L, Torres-Lockhart K, Forster N, Ramakrishnan S, Greninger P, Garnett MJ, et al. Mcl-1 and FBW7 control a dominant survival pathway underlying HDAC and Bcl-2 inhibitor synergy in squamous cell carcinoma. Cancer discovery 2013;3(3):324–37. [PubMed: 23274910]
20. Tong J, Wang P, Tan S, Chen D, Nikolovska-Coleska Z, Zou F, et al. Mcl-1 Degradation Is Required for Targeted Therapeutics to Eradicate Colon Cancer Cells. Cancer Res 2017;77(9): 2512–21. [PubMed: 28202514]
21. Yu J, Wang Z, Kinzler KW, Vogelstein B, Zhang L. PUMA mediates the apoptotic response to p53 in colorectal cancer cells. Proc Natl Acad Sci U S A 2003;100(4):1931–36. [PubMed: 12574499]
22. Abulwerdi F, Liao C, Liu M, Azmi AS, Aboukameel A, Mady AS, et al. A novel small-molecule inhibitor of mcl-1 blocks pancreatic cancer growth in vitro and in vivo. Mol Cancer Ther 2014;13(3):565–75. [PubMed: 24019208]
23. Abulwerdi FA, Liao C, Mady AS, Gavin J, Shen C, Cierpicki T, et al. 3-Substituted-N-(4-hydroxynaphthalen-1-yl)arylsulfonamides as a novel class of selective Mcl-1 inhibitors: structure-based design, synthesis, SAR, and biological evaluation. J Med Chem 2014;57(10):4111–33. [PubMed: 24749893]
24. Zhang X, Guo C, Chen Y, Shulha HP, Schnetz MP, LaFramboise T, et al. Epitope tagging of endogenous proteins for genome-wide ChIP-chip studies. Nature methods 2008;5(2):163–5. [PubMed: 18176569]
25. Peng R, Tong JS, Li H, Yue B, Zou F, Yu J, et al. Targeting Bax interaction sites reveals that only homo-oligomerization sites are essential for its activation. Cell Death Differ 2013;20(5):744–54. [PubMed: 23392123]
26. Wang P, Yu J, Zhang L. The nuclear function of p53 is required for PUMA-mediated apoptosis induced by DNA damage. Proc Natl Acad Sci U S A 2007;104(10):4054–9. [PubMed: 17360476]
27. Dudgeon C, Peng R, Wang P, Sebastiani A, Yu J, Zhang L. Inhibiting oncogenic signaling by sorafenib activates PUMA via GSK3beta and NF-kappaB to suppress tumor cell growth. Oncogene 2012;31:4848–58. [PubMed: 22286758]
28. Ding Q, Xia W, Liu JC, Yang JY, Lee DF, Xia J, et al. Erk associates with and primes GSK-3beta for its inactivation resulting in upregulation of beta-catenin. Mol Cell 2005;19(2):159–70. [PubMed: 16039586]
29. Tong J, Tan S, Zou F, Yu J, Zhang L. FBW7 mutations mediate resistance of colorectal cancer to targeted therapies by blocking Mcl-1 degradation. Oncogene 2017;36(6):787–96. [PubMed: 27399335]
30. Varadarajan S, Vogler M, Butterworth M, Dinsdale D, Walensky LD, Cohen GM. Evaluation and critical assessment of putative MCL-1 inhibitors. Cell Death Differ 2013;20(11):1475–84. [PubMed: 23832116]
31. Soderberg O, Gullberg M, Jarvius M, Ridderstrale K, Leuchowius KJ, Jarvius J, et al. Direct observation of individual endogenous protein complexes in situ by proximity ligation. Nature methods 2006;3(12):995–1000. [PubMed: 17072308]
32. Hanahan D, Weinberg RA. Hallmarks of cancer: the next generation. Cell 2011;144(5):646–74. [PubMed: 21376230]
33. Beroukhim R, Mermel CH, Porter D, Wei G, Raychaudhuri S, Donovan J, et al. The landscape of somatic copy-number alteration across human cancers. Nature 2010;463(7283):899–905. [PubMed: 20164920]
34. Ming L, Wang P, Bank A, Yu J, Zhang L. PUMA dissociates Bax and BCL-XL to induce apoptosis in colon cancer cells. J Biol Chem 2006;281(23):16034–42. [PubMed: 16608847]
35. Czabotar PE, Lee EF, van Delft MF, Day CL, Smith BJ, Huang DC, et al. Structural insights into the degradation of Mcl-1 induced by BH3 domains. Proc Natl Acad Sci U S A 2007;104(15): 6217–22. [PubMed: 17389404]
36. Day CL, Smits C, Fan FC, Lee EF, Fairlie WD, Hinds MG. Structure of the BH3 domains from the p53-inducible BH3-only proteins Noxa and Puma in complex with Mcl-1. J Mol Biol 2008;380(5): 958–71. [PubMed: 18589438]
37. Fire E, Gulla SV, Grant RA, Keating AE. Mcl-1-Bim complexes accommodate surprising point mutations via minor structural changes. Protein science : a publication of the Protein Society 2010;19(3):507–19. [PubMed: 20066663]

38. Day CL, Chen L, Richardson SJ, Harrison PJ, Huang DC, Hinds MG. Solution structure of prosurvival Mcl-1 and characterization of its binding by proapoptotic BH3-only ligands. J Biol Chem 2005;280(6):4738–44. [PubMed: 15550399]

39. Nishi H, Hashimoto K, Panchenko AR. Phosphorylation in protein-protein binding: effect on stability and function. Structure 2011;19(12):1807–15. [PubMed: 22153503]

40. Beltrao P, Bork P, Krogan NJ, van Noort V. Evolution and functional cross-talk of protein post-translational modifications. Molecular systems biology 2013;9:714. [PubMed: 24366814]

41. Betts MJ, Wichmann O, Utz M, Andre T, Petsalaki E, Minguez P, et al. Systematic identification of phosphorylation-mediated protein interaction switches. PLoS computational biology 2017;13(3):e1005462. [PubMed: 28346509]

42. Wang Z, Inuzuka H, Zhong J, Wan L, Fukushima H, Sarkar FH, et al. Tumor suppressor functions of FBW7 in cancer development and progression. FEBS Lett 2012;586(10):1409–18. [PubMed: 22673505]

43. Zhang J, Kan S, Huang B, Hao Z, Mak TW, Zhong Q. Mule determines the apoptotic response to HDAC inhibitors by targeted ubiquitination and destruction of HDAC2. Genes Dev 2011;25(24): 2610–8. [PubMed: 22016339]

44. Del Poeta G, Postorino M, Pupo L, Del Principe MI, Dal Bo M, Bittolo T, et al. Venetoclax: Bcl-2 inhibition for the treatment of chronic lymphocytic leukemia. Drugs of today 2016;52(4):249–60. [PubMed: 27252989]

45. Konopleva M, Contractor R, Tsao T, Samudio I, Ruvolo PP, Kitada S, et al. Mechanisms of apoptosis sensitivity and resistance to the BH3 mimetic ABT-737 in acute myeloid leukemia. Cancer Cell 2006;10(5):375–88. [PubMed: 17097560]

46. Tahir SK, Yang X, Anderson MG, Morgan-Lappe SE, Sarthy AV, Chen J, et al. Influence of Bcl-2 family members on the cellular response of small-cell lung cancer cell lines to ABT-737. Cancer Res 2007;67(3):1176–83. [PubMed: 17283153]

47. van Delft MF, Wei AH, Mason KD, Vandenberg CJ, Chen L, Czabotar PE, et al. The BH3 mimetic ABT-737 targets selective Bcl-2 proteins and efficiently induces apoptosis via Bak/Bax if Mcl-1 is neutralized. Cancer Cell 2006;10(5):389–99. [PubMed: 17097561]

48. Belmar J, Fesik SW. Small molecule Mcl-1 inhibitors for the treatment of cancer. Pharmacol Ther 2015;145:76–84. [PubMed: 25172548]

49. Kotschy A, Szlavik Z, Murray J, Davidson J, Maragno AL, Le Toumelin-Braizat G, et al. The MCL1 inhibitor S63845 is tolerable and effective in diverse cancer models. Nature 2016;538(7626):477–82. [PubMed: 27760111]

Significance

Findings present a novel degradation-independent function of Mcl-1 phosphorylation in anticancer therapy that could be useful for developing new Mcl-1 targeting agents to overcome therapeutic resistance.

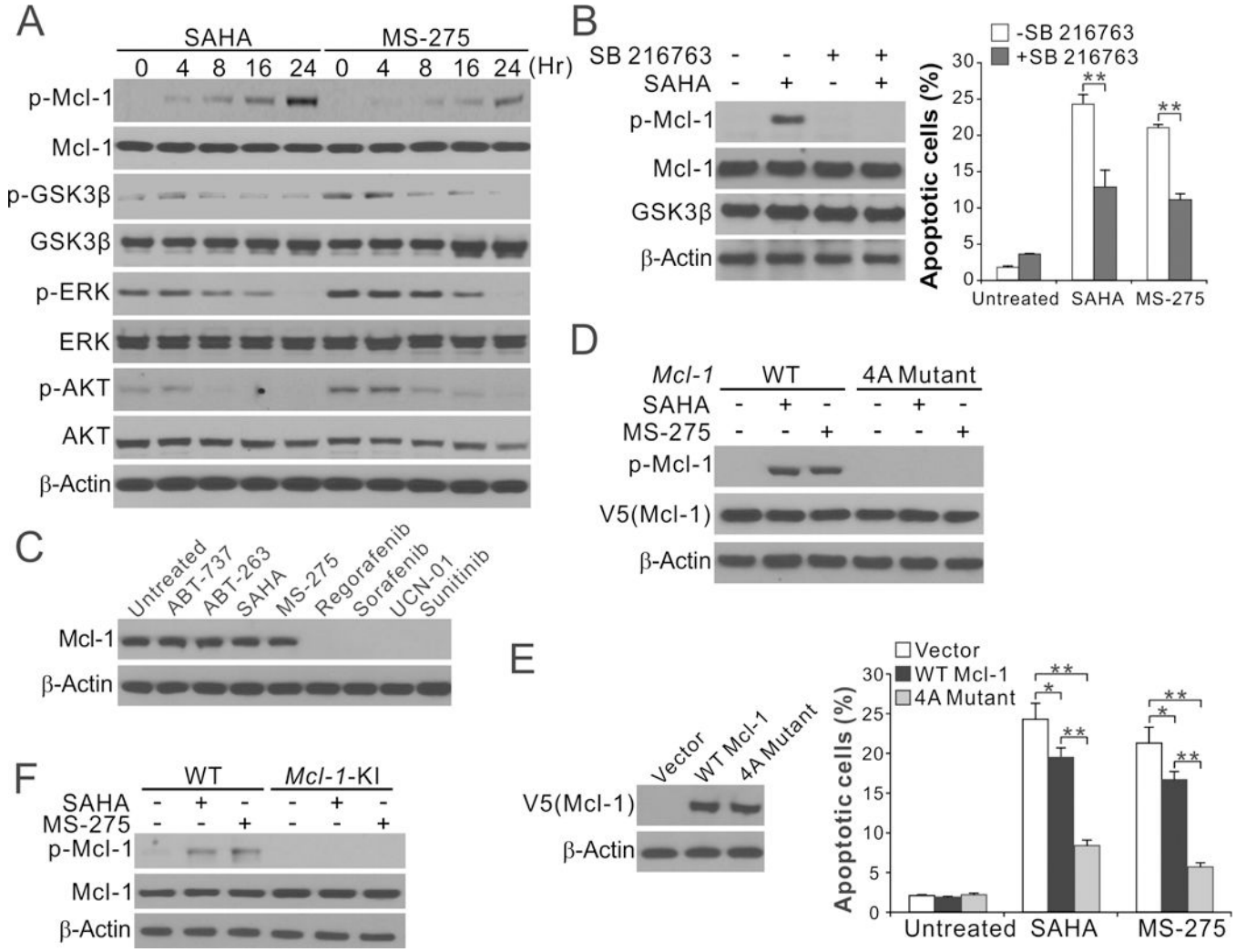

Figure 1. HDAC inhibitors promote GSK3β-mediated Mcl-1 phosphorylation and apoptosis.

(A) Western blotting of indicated proteins in HCT116 cells treated with SAHA or MS-275 at indicated time points. p-Mcl-1: S159/T163; p-GSK3β: S9; p-ERK: T202/Y204; p-AKT: S473. **(B)** HCT116 cells were treated with SAHA with or without the GSK3 inhibitor SB216763 (5 μM) for 24 hr. *Left*, western blotting of indicated proteins; *right*, apoptosis was analyzed by counting condensed and fragmented nuclei after nuclear staining with Hoechst 33258. **(C)** Western blotting of Mcl-1 in HCT116 cells treated with indicated agents for 24 hr. ABT-263: 5 μM; ABT-737: 5 μM; SAHA: 4 μM; MS-275: 5 μM; regorafenib: 40 μM; sorafenib: 20 μM; UCN-01: 1 μM; sunitinib: 15 μM. **(D)** Western blotting of indicated proteins in HCT116 cells transfected with V5-tagged WT or 4A mutant Mcl-1 (S121A/E125A/S159A/T163A) and treated with SAHA or MS-275 for 24 hr. **(E)** Apoptosis in HCT116 cells transfected and treated as in (D) was analyzed as in (B). **(F)** Western blotting of indicated proteins in WT and *Mcl-1* knock-in (*Mcl-1*-KI) HCT116 cells treated with SAHA or MS-275 for 24 hr. In (A)-(F), SAHA: 4 μM; MS-275: 5 μM. In (B) and (E), results were expressed as means ± s.d. of three independent experiments. *****, $P<0.05$; ******, $P<0.01$.

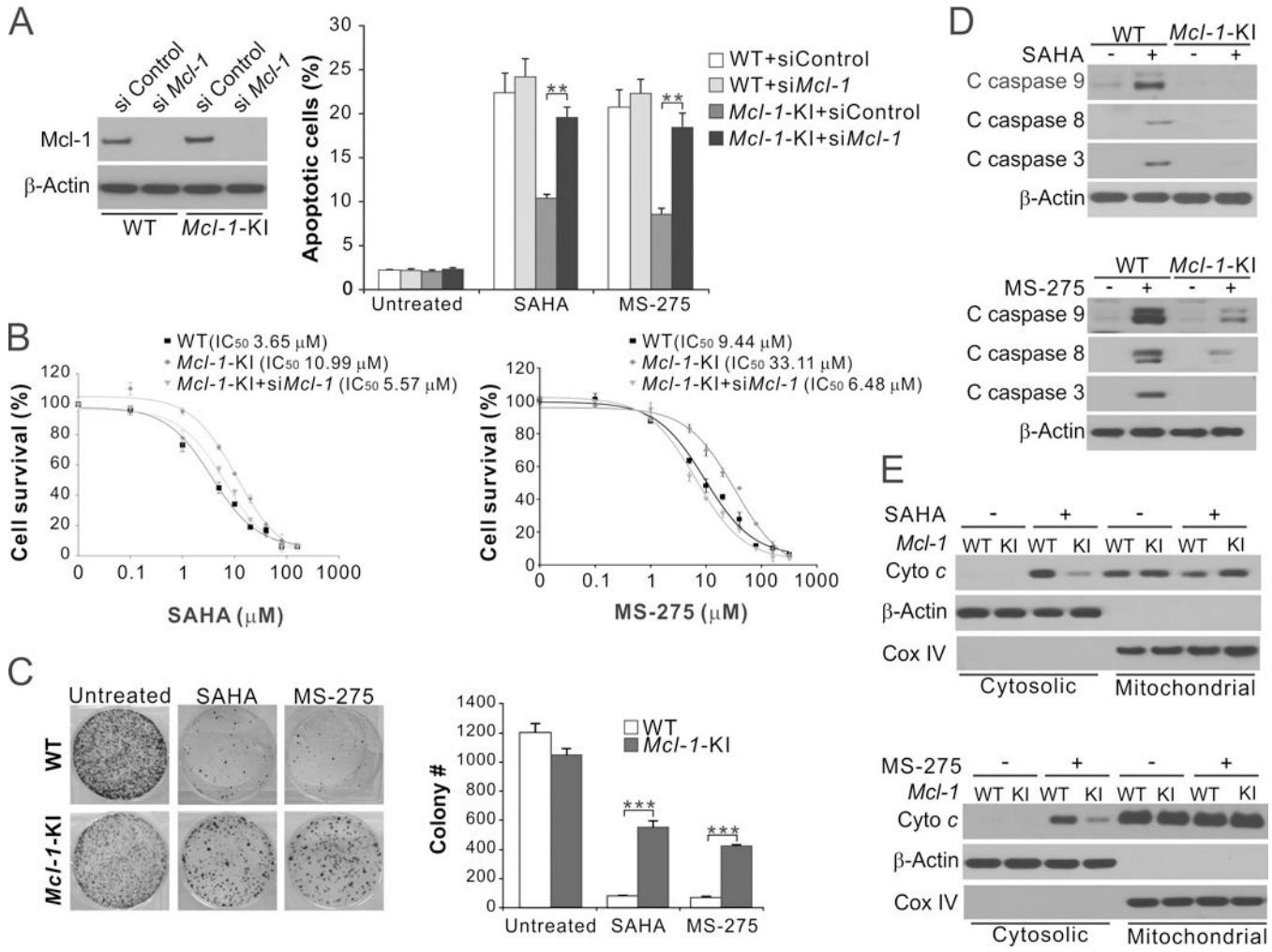

Figure 2. Specifically blocking Mcl-1 phosphorylation suppresses apoptosis induced by HDACi.

(A) WT and *Mcl-1*-KI HCT116 cells transfected with control scrambled or *Mcl-1* siRNA were treated with SAHA or MS-275 for 24 hr. *Left*, western blotting of Mcl-1 knockdown; *right*, apoptosis was analyzed by counting condensed and fragmented nuclei after nuclear staining. **(B)** MTS analysis of viability of WT (black), *Mcl-1*-KI (red) and *Mcl-1*-KI transfected with *Mcl-1* siRNA (green) HCT116 cells treated with SAHA or MS-275 at different concentrations for 72 hr. **(C)** Colony formation assay was done by seeding an equal number of WT and *Mcl-1*-KI HCT116 cells treated with SAHA or MS-275 for 24 hr in 12-well plates, and staining of the attached cells with crystal violet after 14 days. *Left*, representative pictures of colonies; *right*, enumeration of colony numbers. ***, $P < 0.001$. **(D)** Western blotting of cleaved (C) caspases 3, 8 and 9 in WT and *Mcl-1* KI HCT116 cells treated with SAHA or MS-275 for 24 hr. **(E)** Cytochrome *c* release in cells treated with SAHA or MS-275 was analyzed by western blotting of mitochondrial or cytosolic fractions isolated from treated cells. β-Actin and cytochrome oxidase subunit IV (COX IV) were used as controls for loading and fractionation. In (A) and (C)-(E), SAHA: 4 μM; MS-275: 5 μM. In (A)-(C), results were expressed as means ± s.d. of three independent experiments. **, $P < 0.01$; ***, $P < 0.001$.

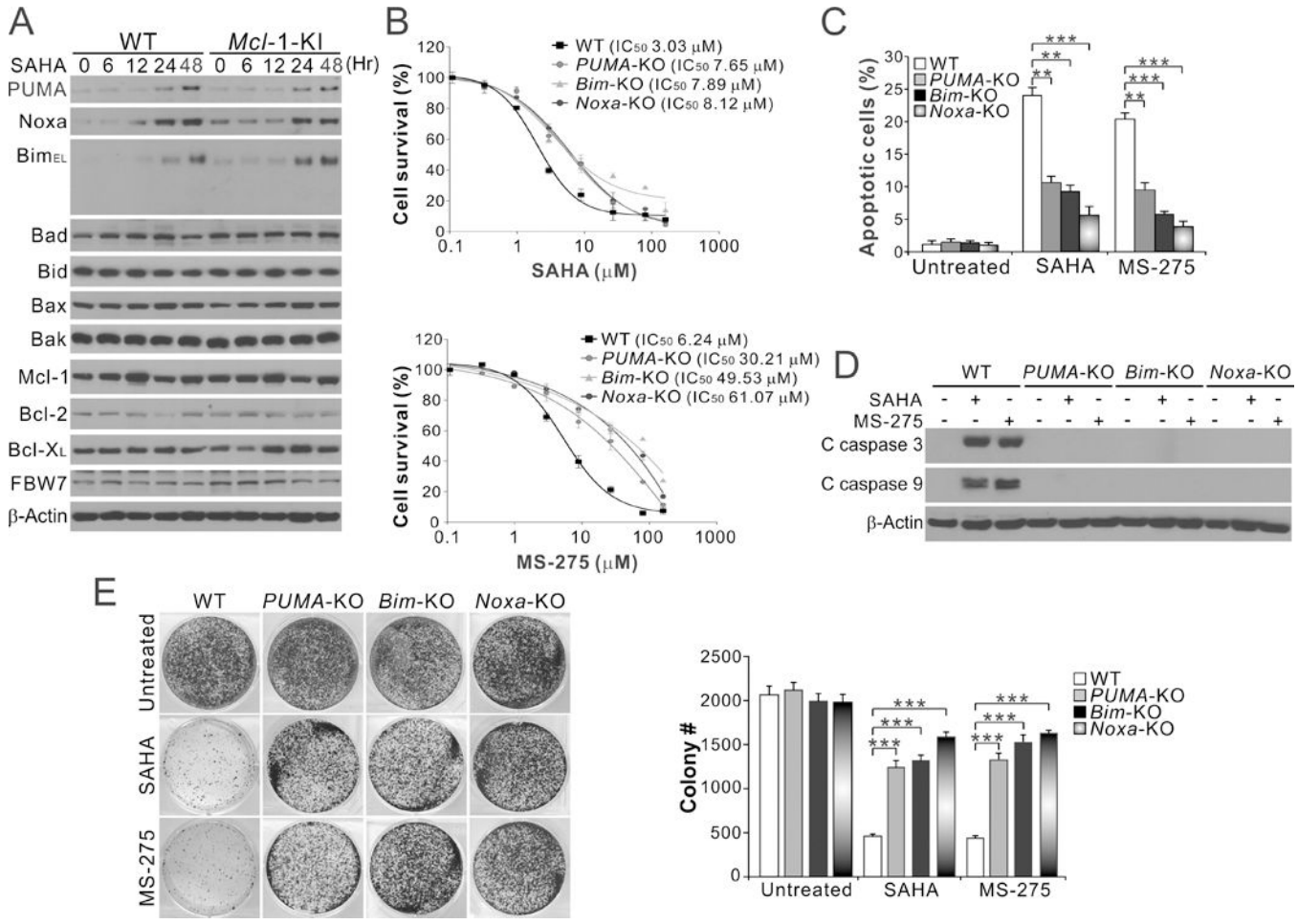

Figure 3. PUMA, Bim and Noxa are required for HDACi-induced apoptosis.

(A) Western blotting of indicated protein in WT and *Mcl-1*-KI HCT116 cells treated with SAHA at indicated time points. **(B)** MTS analysis of WT (black), *PUMA*-KO (red), *Bim*-KO (green) and *Noxa*-KO (blue) HCT116 cells treated with SAHA at different concentrations for 72 hr. **(C)** Apoptosis in the indicated cells treated with SAHA or MS-275 for 24 hr was analyzed by counting condensed and fragmented nuclei after nuclear staining. **(D)** Western blotting of cleaved (C) caspases 3 and 9 in the cells treated as in (C). **(E)** Colony formation of the cells treated as in (C) was analyzed by crystal violet staining. *Left*, representative pictures of colonies; *right*, enumeration of colony numbers. In (A), (C), (D) and (E), SAHA: 4 μM; MS-275: 5 μM. In (B), (C) and (E), results were expressed as means ± s.d. of three independent experiments. ******, $P<0.01$; *******, $P<0.001$.

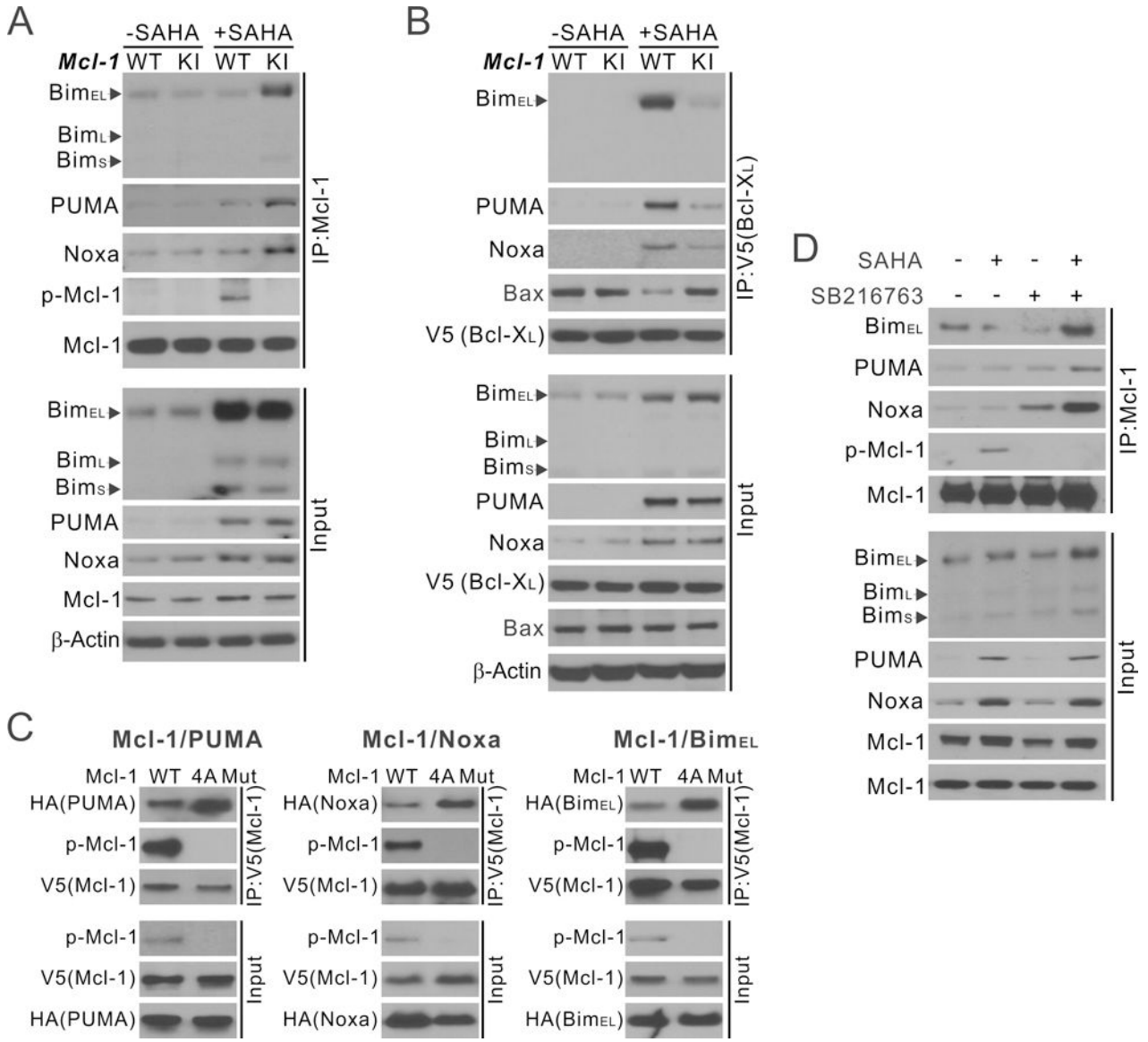

Figure 4. Phosphorylation-dead Mcl-1 binds to PUMA, Bim and Noxa to block apoptosis induced by HDACi.

(A) WT and *Mcl-1*-KI HCT116 cells were treated with 4 μM SAHA for 24 hr. Mcl-1 was immunoprecipitated (IP) followed by western blotting of indicated proteins. p-Mcl-1: S159/T163. **(B)** WT and *Mcl-1*-KI HCT116 cells transfected with V5-Bcl-X_L were treated with 4 μM SAHA for 24 hr. V5 (Bcl-X_L) IP was performed followed by western blotting of indicated proteins. **(C)** HCT116 cells were co-transfected with V5-Mcl-1 (WT or 4A mutant), along with HA-PUMA, HA-Noxa, or HA-Bim. V5 (Mcl-1) IP was performed followed by western blotting of indicated proteins or tags. **(D)** HCT116 cells were treated with 4 μM SAHA with or without the GSK3 inhibitor SB216763 (5 μM) for 24 hr. Mcl-1 IP was performed followed by western blotting of indicated proteins.

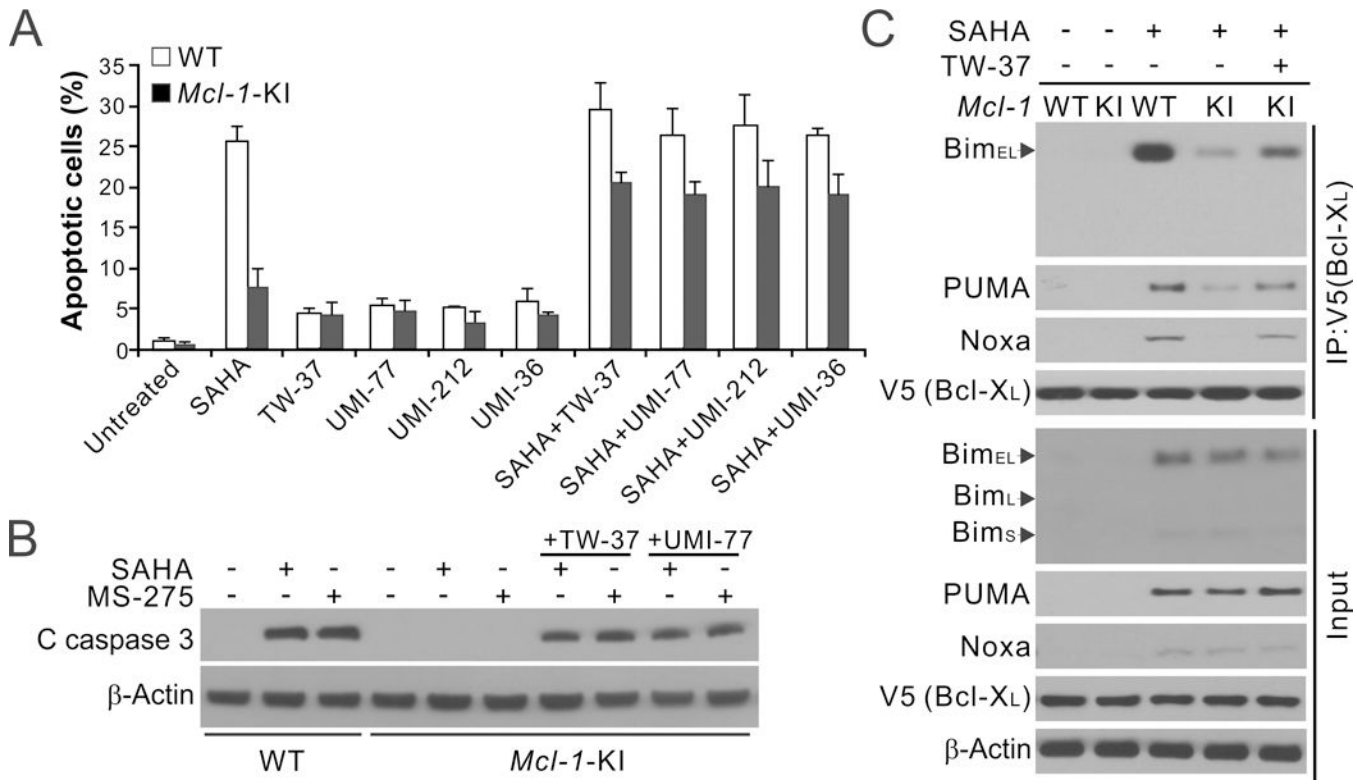

Figure 5. Mcl-1 inhibitors restore HDACi sensitivity by relieving PUMA, Bim and Noxa.

(A) Apoptosis in WT and *Mcl-1*-KI HCT116 cells treated with SAHA with or without a combination with 5 μM UMI-77, UMI-212, UMI-36 or TW-37. Results were expressed as means ± s.d. of three independent experiments. **(B)** Western blotting of cleaved (C) caspase 3 in WT and *Mcl-1*-KI HCT116 cells treated with SAHA or MS-275 with or without a combination with 5 μM TW-37 or UMI-77 for 24 hr. **(C)** WT and *Mcl-1*-KI HCT116 cells transfected with V5-Bcl-X_L were treated with SAHA with or without a combination with 5 μM TW-37 for 24 hr. V5 (Bcl-X_L) IP was performed followed by western blotting of indicated proteins. In (A)-(C), SAHA: 4 μM; MS-275: 5 μM.

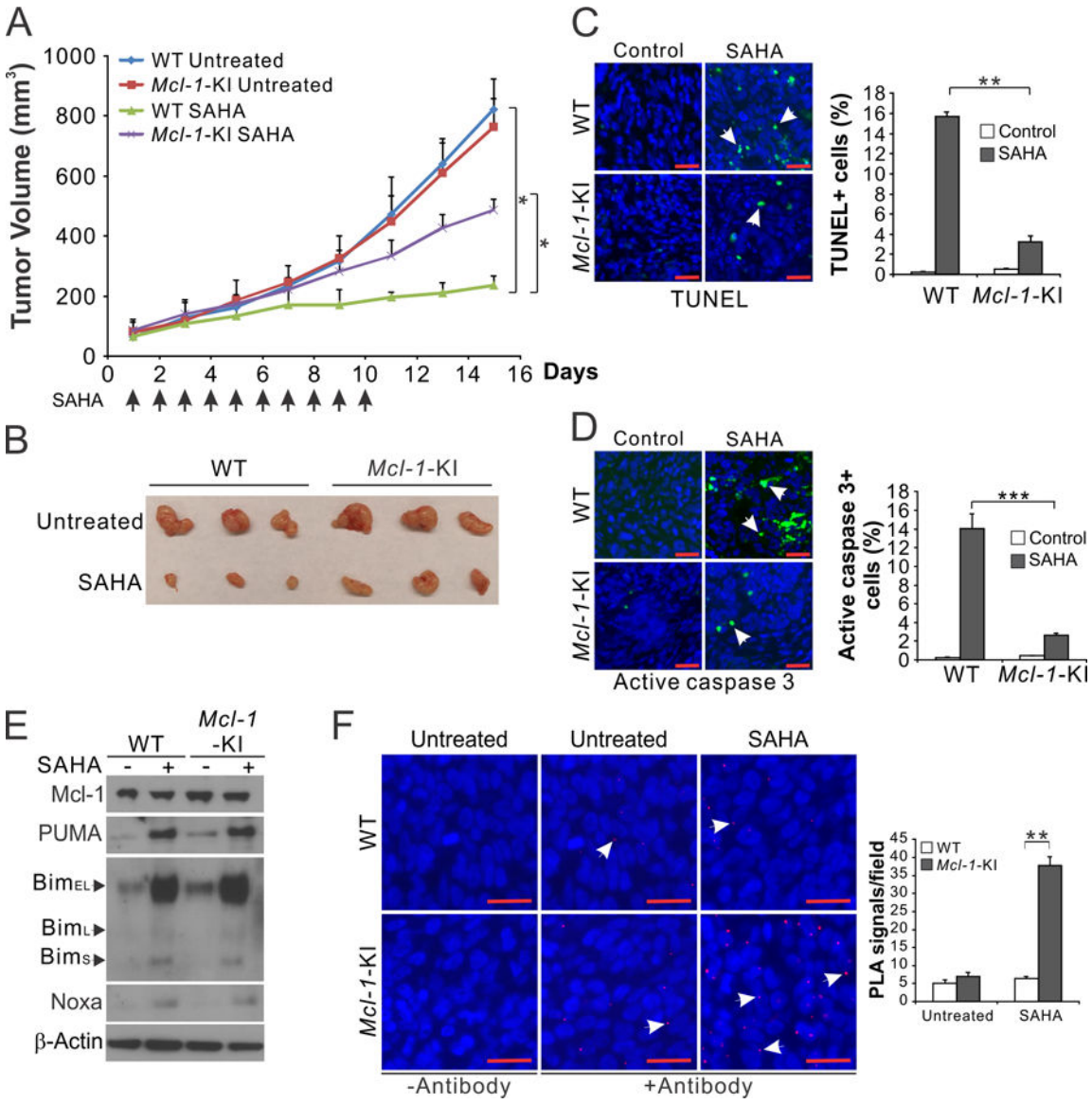

Figure 6. Mcl-1 phosphorylation mediates the antitumor effects of HDACi *in vivo*.

(A) Nude mice with established WT or *Mcl-1*-KI HCT116 xenografts were treated with 50 mg/kg SAHA daily by i.p. injection (indicated by arrows), or the vehicle control for 10 consecutive days. Tumor volume at indicated time points after treatment was plotted with statistical significance for indicated comparisons (n=5 in each group). **(B)** Representative tumors at the end of the experiment. **(C)**, **(D)** Nude mice with WT or *Mcl-1*-KI HCT116 tumors were treated with SAHA as in (A) for 4 consecutive days. Tissue sections were analyzed for apoptosis by TUNEL (C) and active caspase 3 (D) staining. *Left*, representative staining pictures; *right*, quantification of TUNEL- and active caspase-3-positive cells. **(E)** Nude mice with WT or *Mcl-1*-KI HCT116 xenografts were treated with SAHA as in (A) for 4 consecutive days. Indicated proteins in randomly selected tumors were analyzed by western blotting. **(F)** Tissue sections from WT or *Mcl-1*-KI HCT116 xenograft tumors treated with SAHA as in (A) for 1 day were analyzed by proximity ligation assay (PLA) to

detect the interaction of PUMA and Mcl-1. *Left*, representative PLA pictures; no primary antibody was included as negative controls; *right*, quantification of PLA signals per field. In (C), (D) and (F), arrows indicate example cells with positive staining. Results were expressed as means ± s.d. of three independent experiments. Scale bars, 25 μm; **, $P<0.01$; ***, $P<0.001$.

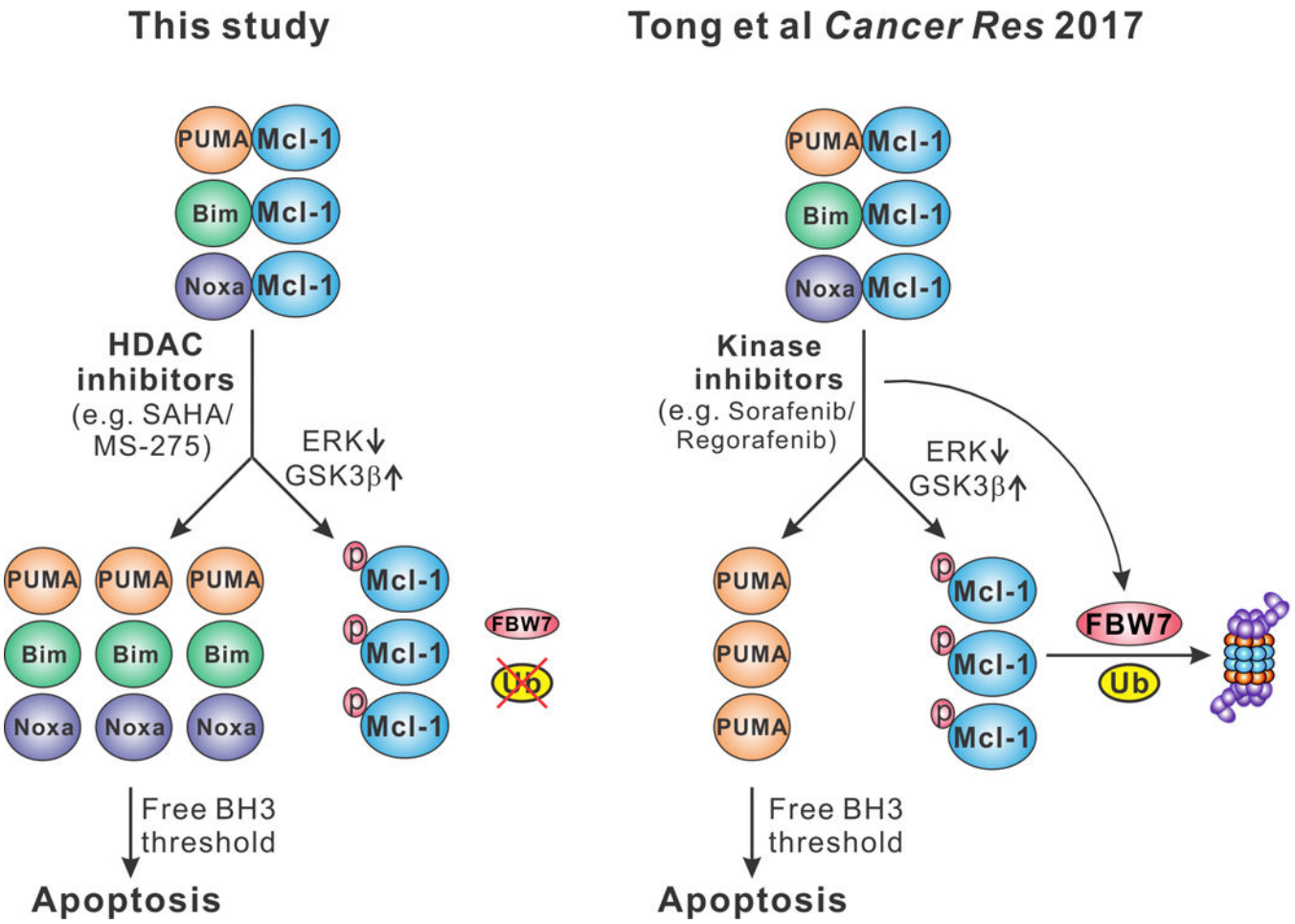

Figure 7. A proposed model for the roles of Mcl-1 phosphorylation in apoptosis induced by HDACi and kinase inhibitors.

ERK inhibition leads to GSK3β-mediated Mcl-1 phosphorylation to promote apoptosis via BH3 liberation (left) and/or FBW7-mediated Mcl-1 degradation (Right).